J Therm Spray Tech
https://doi.org/10.1007/s11666-024-01825-0

ORIGINAL RESEARCH ARTICLE

Effect of Porosity on Abradability of YSZ Coatings

Dan Guo[1,2,3] · Xiaolei Hu[1,2,3] · Jianming Liu[1,2,3] · Tong Liu[1,2,3]

Submitted: 14 May 2024 / in revised form: 7 July 2024 / Accepted: 12 July 2024

Abstract The effect of porosity on the wear behavior of YSZ abradable coating under simulated working conditions was studied using the high-temperature and ultra-high-speed abradability test rig. The results show that the porosity significantly influences the macroscopic morphology and abradability of the YSZ coating at the experimental temperatures of 1000 °C, with the blade tip velocity of 350 m/s, and the feed rate of 50 μm/s. The wear degree of the blade gradually decreases as porosity increases, and the incursion depth ratio (IDR) dramatically decreases. When the porosity reaches its maximum value, the wear scar of the coating is smoothest, and there is no discernible wear on the blade, the IDR value reaches its minimum, and the abradability of the coating reaches its maximum. Besides, brittle fracture in the YSZ coating with high porosity is concluded to be the reason for better abradability.

Keywords abradability · porosity · seal coating · simulated working conditions · YSZ

✉ Dan Guo
gdan1994@163.com

[1] BGRIMM Advanced Materials Science & Technology Co., Ltd, Beijing 102206, China

[2] BGRIMM Technology Group, Beijing 102206, China

[3] Beijing Engineering Technology Research Center of Surface Strengthening and Repairing of Industry Parts, Beijing 102206, China

Introduction

High thrust, high efficiency, and low fuel consumption are the main objectives of aviation engine design and production. Therefore, it is essential to increase the inlet gas temperature of the turbine engine and reduce the gap between the rotor and stator components (Ref 1). Abradable seal coatings have achieved great success in this regard and are currently widely employed in turbo generators for land-based turbo generators and aero-engines (Ref 2-5). With the continuous increase of gas temperature in the turbine (above 1000 °C), the abradable seal coating must possess excellent high-temperature resistance and good abradability (Ref 6-8). However, metal-based seal coatings have poor high-temperature oxidation resistance and face serious problems such as sintering hardening and peeling (Ref 9-11). Ceramic-based seal coatings, with their advantages of higher heat resistance temperatures, have become one of the key technical solutions for advanced engines (Ref 12-14). The ceramic phase has several advantages, including high melting point, phase stability, oxidation resistance, and corrosion resistance. However, this coating is characterized by high hardness and poor wear resistance. If used directly as a seal coating, it can damage turbine blades. (Ref 15, 16)

Yttrium-stabilized zirconia (YSZ) ceramic has become a commonly used high-temperature seal coating for engines due to its excellent comprehensive properties, such as low thermal conductivity, low thermal expansion, excellent thermal shock resistance and high melting point (Ref 17). Some studies have reported on the preparation and characterization of YSZ coatings (Ref 18-22). Atmospheric plasma spraying (APS) is one of the promising methods for preparing YSZ coating. The porosity and pore size of the coating can be adjusted by modifying the process

Published online: 08 August 2024

parameters of plasma spray, such as spraying power, current, and spraying distance. These adjustments directly impact the performance of the YSZ coating.

The research on the wear process of seal coating is currently a popular area of research. The main focus of development in this field is to conduct experimental research using abradability test rig that simulate the high-temperature and high-speed working conditions of aircraft engines (Ref 23). Compared to basic performance, studying the abradability of YSZ coatings with varying porosity under simulated operating conditions is valuable for the design and practical application of YSZ coatings. However, there is very little research on this aspect in existing research.

In this study, five YSZ abradable coatings with different porosity were selected for abradability test by a high-temperature and high-speed rig. The coating abradability related to their porosity was investigated.

Materials and Methods

INCONEL 718 was selected as the substrate material for the experiment, and MCrAlY powder and YSZ powder, developed by BGRIMM Technology Group, were used for the bond and top coatings, respectively. The morphology of YSZ powder is shown in Fig. 1, consisting of nearly spherical particles. The chemical composition of the powder is shown in Table 1.

The bond coating was prepared using low-pressure plasma spraying system (LPPS-TF, Oerlikon Metco, USA). Before spraying, the surface of the sample was cleaned with acetone, and white corundum (850 μm) was used for roughening treatment by sandblasting. After spraying, the samples were subjected to heat treatment under vacuum at 1050 °C for 2 hours and then allowed to cool at 25 °C for 2 hours. The YSZ top coating was prepared using the high-energy plasma spraying system (DELTA, GTV, Germany), and the powder was dried before spraying. This study prepared YSZ coatings with varying porosity by adjusting spray parameters, as indicated in Table 2.

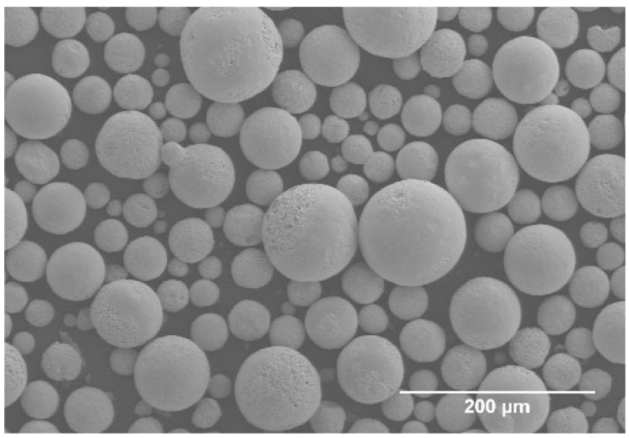

Fig. 1 Morphology of YSZ powder

The high-temperature and ultra-high-speed abradability test is currently the closest evaluation method internationally adopted to simulate the actual working conditions of aviation engines. This method evaluates coatings and studies the wear mechanism by simulating the mutual scraping process between dynamic and static components. The high-temperature and high-speed abradability test rig (BGRIMM-ATR, BGRIMM Technology Group, China) (Fig. 2) has a maximum disc speed of 15500 rpm, a maximum linear speed of 450 m/s, a maximum test temperature of 1200 °C, and a feed rate of 2-2000 μm/s. The MCrAlY-based blade tip wear-resistant coating, prepared by BGRIMM Technology Group, has been selected for coating the grinding blade tips, the thickness is 0.2 mm. The abradability test parameters of YSZ coatings with varying porosity are presented in Table 3. (The number of test groups for YSZ coatings with each porosity is 3).

The abradability of the coating is quantitatively evaluated using the Incursion Depth Ratio (IDR) (Ref 24). The IDR is defined as the ratio of the change in blade height before and after the test to the total feed depth.

$$IDR = \begin{cases} \dfrac{\Delta h}{D} (\Delta h < 0) \\ \dfrac{\Delta h}{D + \Delta h} (\Delta h > 0) \end{cases} \quad \text{(Eq 1)}$$

Where Δh represents the height variation value of the blade, and D denotes the scratch depth of the coating (Ref 25). When blade wear is the main factor, IDR is positive, and when the coating material adheres to the blade, IDR is negative. The smaller the absolute value of IDR, the better the abradability. In general, when the absolute value of the IDR is less than 10%, the abradability of the coating is considered excellent. When the absolute value of the IDR is between 10 and 20%, the abradability of the coating is considered good, and when the absolute value of the IDR is between 20 and 30%, the abradability of the coating is considered acceptable.

The macroscopic morphology of the coating and blade wear marks after the experiment was analyzed using an optical microscope. Additionally, the microstructure analyses were conducted using a scanning electron microscope (SEM, Hitachi SU5000, 15kV, 10mm) equipped with energy dispersive spectroscope (EDS). The porosity of the

Table 1 Chemical composition of YSZ powder (wt.%)

ZrO_2	Y_2O_3	SiO_2	Al_2O_3	Fe_2O_3	TiO_2	Na_2O	K_2O
92.65	7.25	< 0.1	< 0.1	< 0.1	< 0.1	< 0.1	< 0.1

Table 2 Technological parameters of thermal spraying

Coating	Spraying method	Ar flow rate, L/min	H_2 flow rate, L/min	Powder feed rate, g/min	Power, kW	Spray distance, mm
MCrAlY	LPPS	100-105	10-12	100	70-75	380-420
YSZ	high-energy plasma spraying	50-55	12-16	200	50-60	110-130

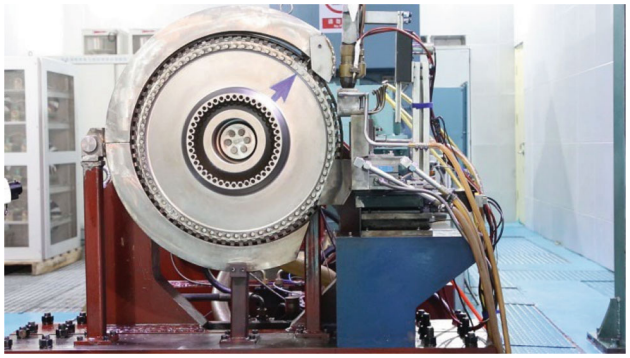

Fig. 2 The image of high-temperature and ultra-high-speed abradability test rig

Table 3 Abradability test parameters

T(°C)	Linear velocity, m/s	Cut Feed, μm/s	Cut Depth, μm
1000	350	50	500

coating was tested using the mercury intrusion method (according to ISO 15901-2005). The mercury solution and pressure gauge were prepared, and a specific amount of mercury solution was poured into the self-supporting coating sample. The pressure of the mercury solution was measured using a pressure gauge, the volume of the mercury solution was calculated based on the density of mercury and the pressure measured by the pressure gauge, the porosity was determined by the ratio of the volume of the mercury solution to the volume of the material, each coating with varying porosity was measured three times, and the average value was calculated from the results.

Results and Discussion

Microscopic Morphology of Coatings with Varying Porosity

YSZ porous abradable coatings with varying porosity were prepared by adjusting spraying parameters, such as spraying distance and powder feeding rate in plasma spraying. The porosity of each coating was measured using the mercury intrusion method. The morphology of YSZ coatings with varying porosity is presented in Fig. 3. The porous YSZ coating consists of ceramic phases and pores. The ceramic phase is light gray, while the pores are uniformly distributed within the ceramic phase and appear black.

Macroscopic Morphology of Coating and Blade After Scraping

Abradability tests were conducted on YSZ coatings with varying porosity. The macroscopic morphology of YSZ coatings and blades after the abradability test is presented in Fig. 4. All coatings have undergone varying degrees of wear, resulting in the appearance of scraped arc-shaped grooves on their surfaces.

Figure 4(a1, a2) shows the YSZ coating with a porosity of 11% and the blade tip. From the figure, it is evident that there is a significant amount of metallic luster substance on the surface of the scratch, which is inferred to be the material transferred to the ceramic surface from the metallic blade during the grinding process. Figure 4(b) and (e) displays the surface morphology of the YSZ coating and the blade tip, revealing a porosity ranging from 18 to 31%. After scraping, the overall surface wear marks appear relatively flat, with consistent scratch patterns. The grinding blades only have shallow grooves with no visible wear, and no serious failures occur. This indicates that the coating can maintain excellent wear resistance even when the porosity exceeds 18%.

Coating Scraping Depth, Blade Wear Height, and Total Wear Depth

The scraping depth and blade wear height of YSZ coating samples with varying porosity after the abradability test were determined. Additionally, the total depth of wear was calculated. Additionally, calculate the total depth of wear. The results are presented in Fig. 5. Under the conditions of a temperature of 1000 °C, a linear speed of 350 m/s, and a feed rate of 50 μm/s, the wear height of the grinding blade gradually decreases as the porosity of the YSZ coating

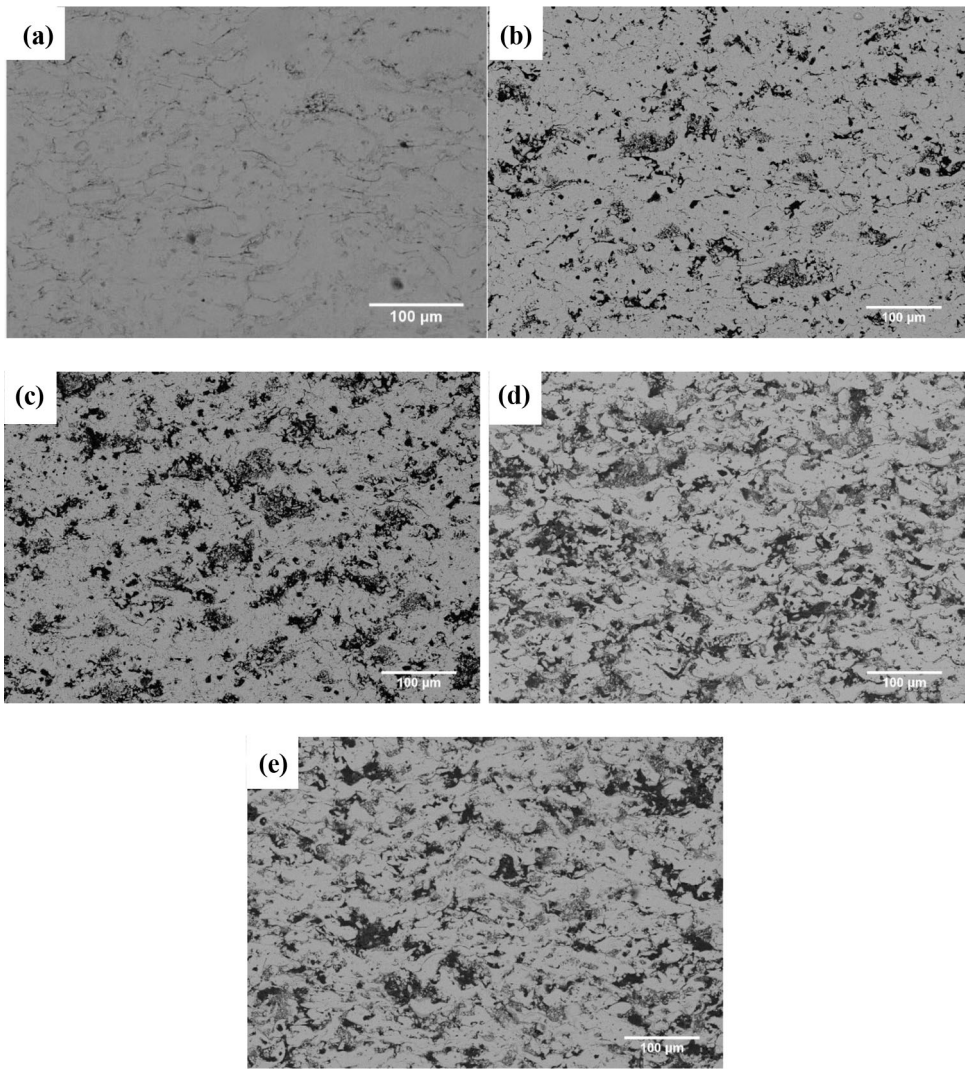

Fig. 3 Morphology of YSZ coating with different porosities of: (a) 11%, (b) 18 %, (c) 24%, (d) 29%, (e) 31%

increases. When the porosity reaches 11%, the wear height of the grinding blade is significantly higher than that of the coating with a porosity between 18 and 31%. Furthermore, when the porosity of the YSZ coating is 11%, the total wear depth in the abradability test is the highest, measuring 1.075 mm. When the porosity ranges from 18 to 31%, the total wear depth ranges from 0.435 to 0.502 mm, indicating a tendency towards stabilization. Based on the morphology of the coating, it can be observed that when the porosity of the YSZ coating is relatively low at 11%, the blades experience severe wear against the coating. Therefore, the total wear depth of the YSZ coating with 11% porosity after the test is significantly higher than that of coatings with higher porosity.

IDR

Based on the results of the abradability test, the IDR values of YSZ coatings with varying porosity were calculated using Eq 1. The relationship between porosity and IDR of the YSZ coating is presented in Fig. 6.

The IDR values of YSZ coatings with varying porosity are all positive. This suggests that blade tip wear occurred under the experimental conditions, leading to a reduction in blade height. It can also be observed that as porosity increases, the absolute value of IDR shows a downward trend. This suggests that the degree of wear on worn blades decreases as the porosity of the YSZ coating increases. This further indicates that the abradability of YSZ coatings improves with the increase in porosity. When the porosity ranges between 11 and 18%, the IDR value significantly decreases with the increase in YSZ coating porosity. When the porosity is between 18 and 31%, the IDR value decreases gradually with the increase in porosity, indicating that the wear resistance of the coating tends to stabilize. From the quantitative analysis of IDR values, it was observed that when the porosity is below 11%, the IDR value exceeds 50%, indicating poor wear resistance.

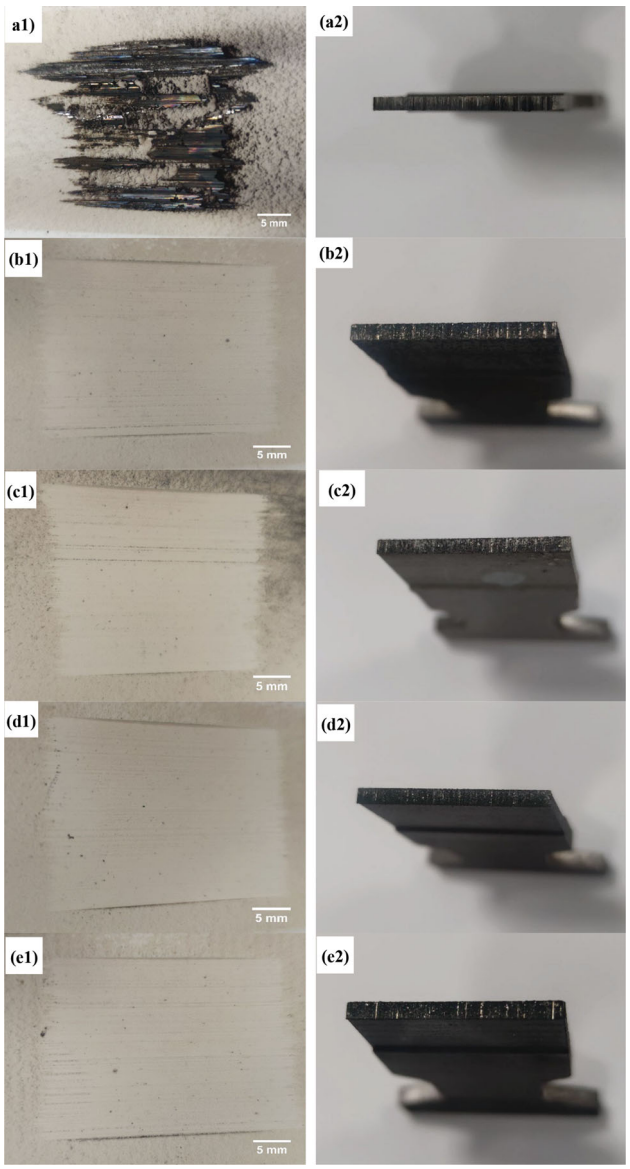

Fig. 4 Optical wear maps of YSZcoating and blade tip: (a1), (a2) 11%; (b1), (b2) 18%; (c1), (c2) 24%; (d1), (d2) 29%, (e1), (e2) 31%

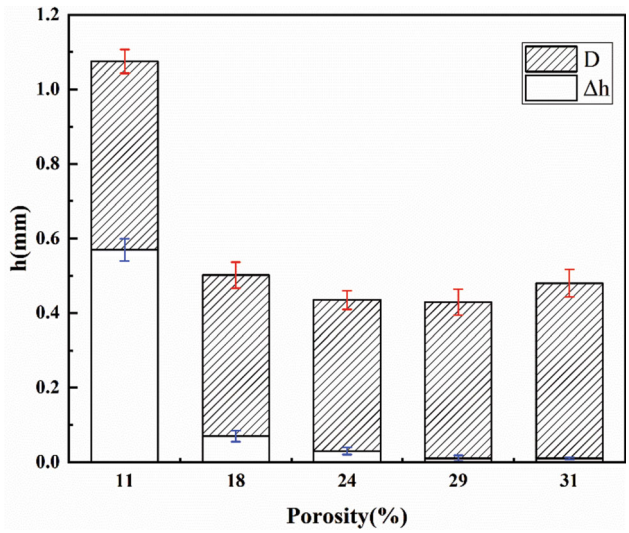

Fig. 5 Scraping depth of the coating (D), wear height (Δ h) of the blade and the total wear depth (D + Δ h)

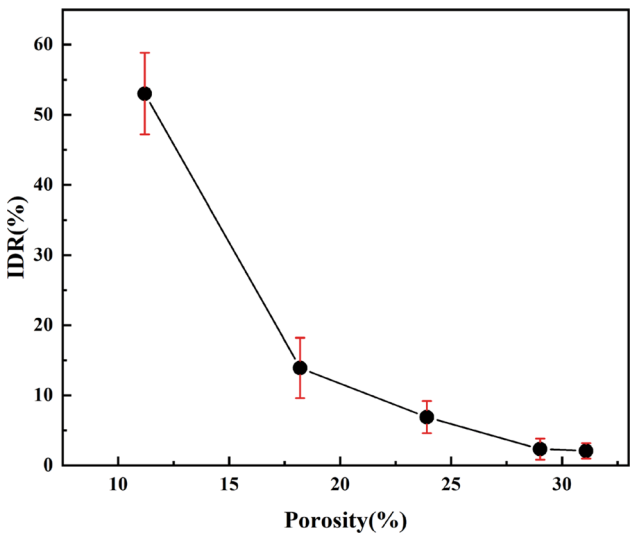

Fig. 6 The relationship between IDR and porosity of YSZ coating

Conversely, when the porosity exceeds 23% and the IDR value is less than 10%, the combination of the abradability of the top ceramic coat and the wear resistance of the metallic counterpart is found to be optimal.

Mechanism Analysis

The microstructure of the YSZ coating with high porosity (31%) was analyzed using SEM (Fig. 7). The micro-morphology of the scratched surface of the coating is predominantly rough, characterized by the presence of "pits" and "pockmarks". This indicates that when the blade invades, a significant number of sprayed particles detach from the surface due to brittle fracture. This confirms that the primary mechanism responsible for the wear of porous YSZ is "micro fracture". Additionally, a few smooth areas were also observed. Combined with the observation of the coating cross-section structure (Fig. 7b), it was found that the original coating structure morphology was well preserved near the scraped surface. No densification or deformation was observed, suggesting that the smooth surface in this area is likely formed through a "cutting" mechanism. Besides, EDS analysis (Fig. 7c) revealed that only the elements of YSZ coating were present on the scratch surface. This indicates the absence of blade tip adhesion during the abradability test process.

When the microstructure of the YSZ coating with low porosity (18%) was analyzed usingSEM (Fig. 8), the scratch surface of the coating showed "adhesive wear"

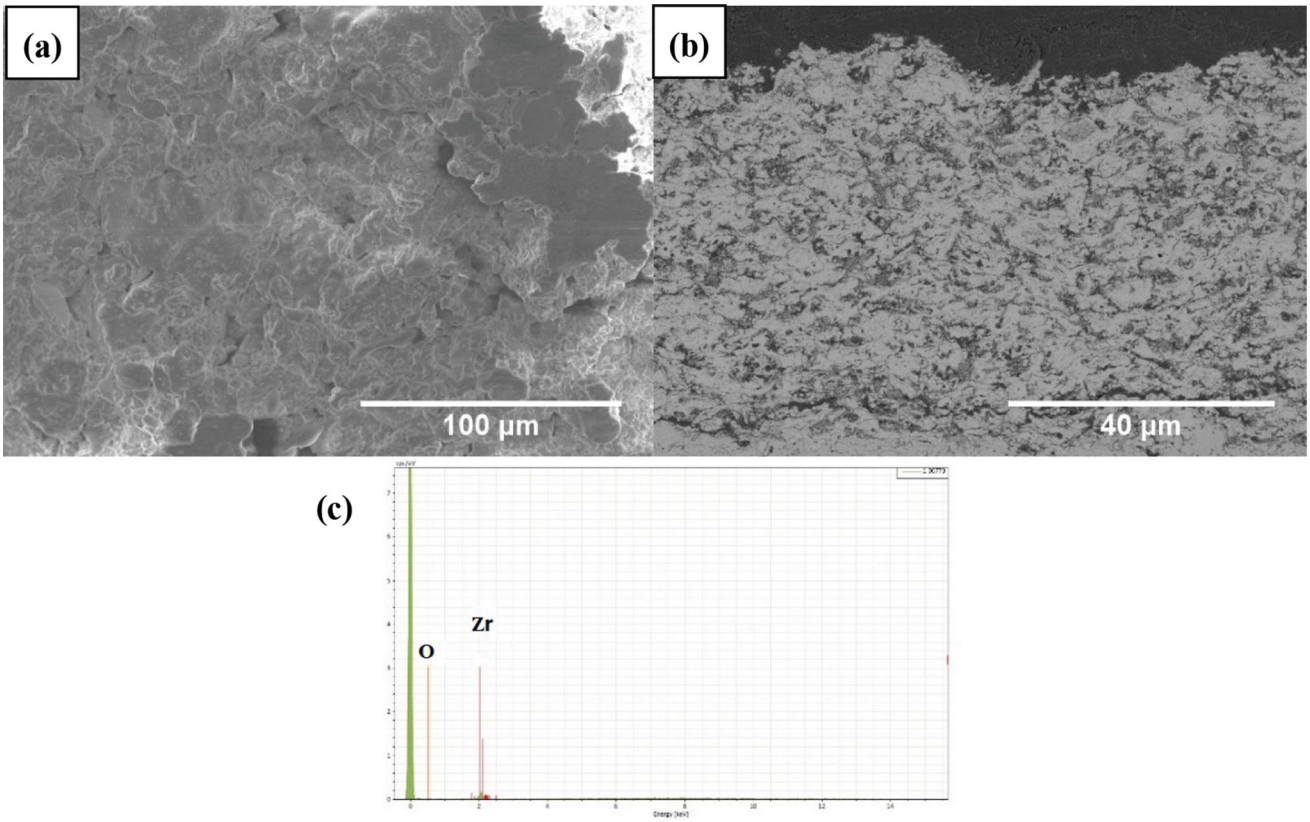

Fig. 7 The scratch microstructure of the YSZ coating with high porosity by SEM: (a) was analyzed using surface, (b) cross-section, (c) energy spectrum analysis at scratches

stripes after the abradability test. Upon examining its cross-sectional structure (Fig. 8b), it was observed that there was a "densification" near the surface of the YSZ coating, with a discontinuous thin adhesive layer on the surface of the YSZ coating. This layer is believed to have formed through the "adhesion transfer" of the blade tip material. Furthermore, energy-dispersive x-ray spectroscopy (EDS) analysis of the scratched surface of the coating after the test (Fig. 8c) revealed the presence of elements like Ti and Ni, which were exclusively found on the scratch surface near the blade tip. This confirms the occurrence of blade tip adhesion to the YSZ coating during the test.

Therefore, the main mechanism for scraping porous YSZ coatings with high porosity is brittle fracture. If this mechanism is effectively utilized, the coating can exhibit excellent abradability. However, the decrease in porosity of the coating makes it more difficult for the "micro-fracture" mechanism to occur. When the blades invade, the coating material does not wear out; instead, it gets compacted and scraped further, leading to significant blade wear and poor abradability performance.

Conclusion

(1) The coating exhibits a burnt black surface in its scraped morphology when the porosity is low. On the other hand, the coating shows uniform and smooth scratches when the porosity is high. Furthermore, as the porosity of the coating increases, the wear on the grinding blades decreases significantly.

(2) When the porosity of the YSZ coating increases, the IDR value decreases significantly. The IDR value gradually decreases as porosity increases between 18 and 31%, indicating that the coating's wear resistance is starting to stabilize.

(3) The maximum level of abradability is indicated when the porosity is 31%, the coating exhibits flat wear marks, and the blades show no discernible wear. The IDR value is 2.08% at this point.

(4) Brittle fracture is the main characteristic that defines the abradable mechanism of porous YSZ coating. Reducing the porosity of the coating may make the "micro-fracture" mechanism more challenging.

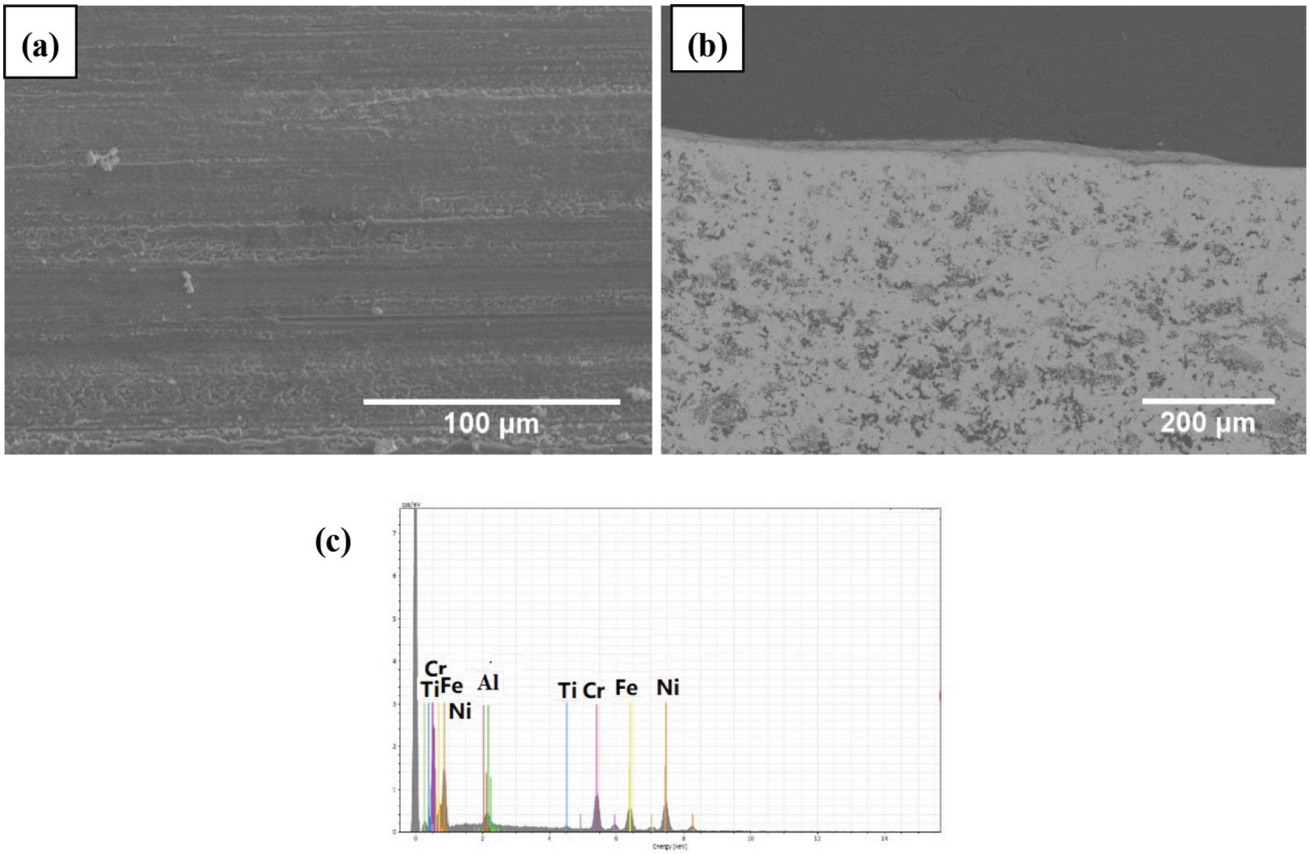

Fig. 8 The scratch microstructure of the YSZ coating with low porosity by SEM: (a) surface, (b) cross section, (c) energy spectrum analysis at scratches

Acknowledgments This work was supported by the National Key R&D Program of China (No. 2022YFB3806300).

References

1. X. Ma and A. Matthews, Investigation of Abradable Seal Coating Performance Using Scratch Testing, *Surf. Coat. Technol.*, 2007, **202**(4), p 1214-1220. https://doi.org/10.1016/j.surfcoat.2007.07.076
2. M. Yi, J. He, B. Huang et al., Friction and Wear Behaviour and Abradability of Abradable Seal Coating, *Wear*, 1999, **231**(1), p 47-53. https://doi.org/10.1016/S0043-1648(99)00093-9
3. P.J. Burnett and D.S. Rickerby, The Mechanical Properties of Wear-Resistant Coatings I Modelling of Hardness Behaviour, *Thin Solid Films*, 1987, **148**(1), p 41-50. https://doi.org/10.1016/0040-6090(87)90119-2
4. Y. Tong, W. Li, Q. Shi, L. Chen, and G. Yang, Self-Lubricating Epoxy-Based Composite Abradable Seal Coating Eliminating Adhesive Transfer via Hierarchical Design, *J. Mater. Sci. Technol.*, 2022, **104**, p 145-154. https://doi.org/10.1016/j.jmst.2021.07.017
5. J. Zhang, X. Lu, J. Lin, L. Ma, and H. Dai, Dynamic Characteristics Analysis of Blade-Casing Rubbing Faults with Abradable Coatings, *Proc. Inst. Mech. Eng., Part C: J. Mech. Eng. Sci.*, 2021, **235**(6), p 975-987. https://doi.org/10.1177/0954406220941553
6. C. Xudong, X. Hongyu, Y.E. Weiping, M. Xiaoming, M. Jie, L. Minzhi et al., Effect of Coated PHB on Properties of Abradable Seal Coating, *J. Wuhan Univ. Technol.-Mater.*, 2014, **29**(3), p 417-421. https://doi.org/10.1007/s11595-014-0932-5
7. M. Aral and T. Suidzu, Porous Ceramic Coating for Transpiration Cooling of Gas Turbine Blade, *J. Therm. Spray Technol.*, 2013, **22**(5), p 690-698. https://doi.org/10.1007/S11666-013-9883-1
8. D. Aussavy, R. Bolot, G. Montavon, F. Peyraut, G. Szyndelman, J. Gurt-Santanach, and S. Selezneff, YSZ-Polyester Abradable Coatings Manufactured by APS, *J. Therm. Spray Technol.*, 2016, **25**(1-2), p 252-263. https://doi.org/10.1007/s11666-015-0358-4
9. X. Gao, J. Hu, and Z.Q. Wang, Numerical Study on Effects of Blade Tip Air Jet on the Flow Field of Wind Turbine Blade Tip, *Hangkong Dongli Xuebao/J. Aerosp. Power*, 2014, **29**(8), p 1863-1870.
10. R. Rajendran, Gas Turbine Coatings—An Overview, *Eng. Fail. Anal.*, 2012, **26**, p 355-369. https://doi.org/10.1016/j.engfailanal.2012.07.007
11. Sporer, D., Dorfman, M., Xie, L., *et al.* Processing and Properties of Advanced Ceramic Abradable Coatings. In Proceedings of the International Thermal Spray Conference and Exposition, Beijing, China, May, 14-16 2007; pp. 143-148.
12. X. Sun, Z. Liu, L. Du et al., A Study on YSZ Abradable Seal Coatings Prepared by Atmospheric Plasma Spray and Mixed Solution Precursor Plasma Spray, *J. Therm. Spray Technol.*, 2021, **30**(5), p 1199-1212. https://doi.org/10.1007/s11666-021-01178-y
13. X. Cheng, Y. Yu, D. Zhang, T. Liu, J. Liu, and J. Shen, Preparation and Performance of an Abradable NiCrFeAlBN-YSZ-

NiCrAl Layered Seal Coating for Aircraft Engines, *J. Therm. Spray Technol.*, 2020, **29**(7), p 1804-1814. https://doi.org/10.1007/s11666-020-01082-x
14. Z. Wang, L. Du, H. Lan, C. Huang, and W. Zhang, Preparation and Characterization of YSZ Abradable Sealing Coating Through Mixed Solution Precursor Plasma Spraying, *Ceram. Int.*, 2019, **45**(9), p 11802-11811. https://doi.org/10.1016/j.ceramint.2019.03.058
15. Y. Gao, J. Gao, D. Yang, and Y. Deming, Equiaxed and Porous Thermal Barrier Coatings Deposited by Atmospheric Plasma Spray Using a Nanoparticles Powder, *Adv. Eng. Mater.*, 2014, **16**(4), p 406-412. https://doi.org/10.1002/adem.201300284
16. C. Lamuta, G. Di Girolamo, and L. Pagnotta, Microstructural, Mechanical and Tribological Properties of Nanostructured YSZ Coatings Produced with Different APS Process Parameters, *Ceram. Int.*, 2015, **41**(7), p 8904-8914. https://doi.org/10.1016/j.ceramint.2015.03.148
17. P. Carpio, M.D. Salvador, R. Benavente, M. Miranda, and E. Sánchez, Impact of Feedstock Nature on Thermal Conductivity of YSZ Thermal Barrier Coatings Obtained by Plasma Spraying, *J. Ceram. Sci. Technol.*, 2016, **7**, p 307-312. https://doi.org/10.4416/JCST2016-00022
18. U. Bardi, C. Giolli, A. Scrivani, G. Rizzi, F. Borgioli, A. Fossati et al., Development and Investigation on New Composite and Ceramic Coatings as Possible Abradable Seals, *J. Therm. Spray Technol.*, 2008, **17**(5-6), p 805-811. https://doi.org/10.1007/s11666-008-9246-5
19. X.M. Sun, L.Z. Du, H. Lan, H.F. Zhang, R.Y. Liu, Z.G. Wang, S.G. Fang, C.B. Huang, Z.A. Liu, and W.G. Zhang, Study on Thermal Shock Behavior of YSZ Abradable Sealing Coating Prepared by Mixed Solution Precursor Plasma Spraying, *Surf. Coat. Technol.*, 2020, **39**, p 126045. https://doi.org/10.1016/j.surfcoat.2020.126045
20. X. Ren, S. Guo, M. Zhao, and W. Pan, Thermal Conductivity and Mechanical Properties of YSZ/$LaPO_4$ Composites, *J. Mater. Sci.*, 2014, **49**(5), p 2243-2251. https://doi.org/10.1007/s10853-013-7919-z
21. Y. Cui, M. Guo, C. Wang, J. Jiao, and L. Cheng, Zirconia-Based Abradable Coatings Fabricated on Single-Crystal Superalloy: Microstructure, Residual Stress and Mechanical Properties, *J. Alloys Compnd.*, 2022, **907**, p 164537. https://doi.org/10.1016/j.jallcom.2022.164537
22. A. Rawaid, H. Taihong, S. Peng, Z. Defeng, A. Shabir, A. Muhammad, A. Syed, H. Dadallah, and L. Jiansheng, Tribological Performance and Phase Transition of MAX-Phase/YSZ Abradable Seal Coating Produced by Air Plasma Spraying, *Ceram. Int.*, 2022, **48**(3), p 4188-4199. https://doi.org/10.1016/j.ceramint.2021.10.210
23. J. Stringer and M.B. Marshall, High speed wear testing of an abradable coating, *Wear*, 2012, **294**, p 257-263. https://doi.org/10.1016/j.wear.2012.07.009
24. R. Schmid. New high temperature abradables for gas turbines. Swiss Federal Institute of Technology (1997)
25. Y.D. Liu, J.P. Zhang, Z.L. Pei, J.H. Liu, W.H. Li, J. Gong, and C. Sun, Investigation on High-Speed Rubbing Behavior Between Abrasive Coatings and Al/hBN Abradable Seal Coatings, *Wear*, 2020 https://doi.org/10.1016/j.wear.2020.203389